J Mater Sci: Mater Med (2015) 26:1
DOI 10.1007/s10856-014-5323-0

Electrochemical behavior and corrosion resistance of Ti–15Mo alloy in naturally-aerated solutions, containing chloride and fluoride ions

A. V. Rodrigues · N. T. C. Oliveira · M. L. dos Santos · A. C. Guastaldi

Received: 28 October 2013 / Accepted: 25 May 2014 / Published online: 11 January 2015

Abstract The electrochemical behavior and corrosion resistance of Ti–15Mo alloy to applications as biomaterials in solutions 0.15 mol L^{-1} Ringer, 0.15 mol L^{-1} Ringer plus 0.036 mol L^{-1} NaF and 0.036 mol L^{-1} NaF (containing 1,500 ppm of fluoride ions, F^-) were investigated using open-circuit potential, cyclic voltammetry, and electrochemical impedance spectroscopy techniques, X-ray photoelectron spectroscopy and scanning electron microscope. Corrosion resistance and electrochemical stability of the Ti–15Mo alloy decreased in solutions containing F^- ions. In all cases, there were formation and growth of TiO_2 and MoO_3 (a protector film), not being observed pitting corrosion, which might enable Ti–15Mo alloys to be used as biomedical implant, at least in the studied conditions, since the electrochemical stability and corrosion resistance of the passive films formed are necessary conditions for osseointegration.

1 Introduction

Nowadays there has been an increase in the utilization of fluoride-containing prophylactic gels and bucal rinses in the dentistry area [1, 2]. Many commercially available fluoride-containing gels contain concentrations of fluoride ions, approximately 10,000 ppm (1 wt%), with a pH, between 7.0 and 3.5 [1, 2].

A high concentration of fluoride ions in the media would influence the corrosion resistance of the Ti and Ti alloys. If the medium is acidic and contains appreciable amounts of fluoride ions, there will be the formation of hydrofluoric acid and, in that situation, the passive film formed on the alloys surface might be attacked, as well as their mechanical properties could be changed [1–4]. Physiological media containing ions such as fluoride and chloride could break the oxide film formed and cause pitting corrosion [3, 4]. The negative influence of fluoride on the corrosion of titanium and its alloys has been reported [2–5]. Ti–30Cu–10Ag, Ti–0.5Pd and Ti–0.5Pt alloys offer a better corrosion resistance than CP–Ti, Ti–6Al–7Nb and Ti–6Al–4V alloys in presence of fluoride since the presence of Ag, Cu, Pd, and Pt in these alloys have the ability to promote passivation [6–8]. Although, studies report that the liberations of small amounts of alloy elements can cause cytotoxic effects to the human body and lead to adverse reactions when it presents elastic modulus incompatible to that from the bone. It might cause stress shield between the implant and the bone, causing bone resorption and premature fails in the implant [9–12].

An oxide film is formed spontaneously on these alloys surface, which consists mainly of amorphous TiO_2. This film will protect the implant against corrosion processes, and its physic-chemical and electrochemical properties, besides its stability in physiological media that has a decisive role on the implants biocompatibility [13, 14].

Actually, several Ti alloys have been developed, such as Ti–Mo, Ti–Nb, Ti–Ta, Ti–Zr and Ti–Hf, and, as they have biocompatible elements and show better mechanical properties than cp-Ti and Ti–6Al–4V, they can be expected to become promising candidates for biomedical and dental applications [15].

Ti–Mo alloys are able biomaterials that can be used in dental implants and biomedical devices. The high corrosion resistance of Ti–Mo alloys is due to the presence of Mo in

A. V. Rodrigues · N. T. C. Oliveira · M. L. dos Santos · A. C. Guastaldi (✉)
Universidade Estadual Paulista "Júlio de Mesquita Filho" - UNESP Campus de Araraquara, Instituto de Química, Araraquara, SP CEP 14800-900, Brazil
e-mail: guastald@iq.unesp.br

their composition and in oxide film surface [15–17]. According to Oliveira and Guastaldi [4, 18] and Oliveira et al. [16] have reported the ability of Ti–Mo alloys having 4–20 wt% Mo to exhibit spontaneous passivation in Ringer's solution and to prevent pitting at potentials up to 8 V [vs. saturated calomel electrode (SCE)]. Oliveira and Guastaldi [4, 18] have suggested Ti–Mo alloys as a suitable biomaterial due to ability to exhibit spontaneous passivation, high electrochemical stability of the passive films formed and excellent biocompatibility. According to Alves et al. [19], both Ti–10Mo and Ti–6Al–4V alloys exhibit similar electrochemical characteristics in 0.15 M NaCl containing 0.03 M NaF, the passive current density is relatively lower for Ti–10Mo alloy.

The behavior of Ti alloys in simulated physiological media can be studied by electrochemical techniques, such as open-circuit potential (E_{oc}), potentiodynamic polarization, cyclic voltammetry (CV) and electrochemical impedance spectroscopy (EIS), which can be used to study the influence of Mo in the corrosion resistance of the passive film, metal alloy oxidation or dissolution of the oxide film formed on the alloy surface [14–17].

The goal of the present study was to investigate the electrochemical behavior and corrosion resistance of biomedical Ti–15Mo alloy in naturally-aerated solutions, containing chloride and fluoride ions.

2 Experimental

Samples of Ti–15Mo (wt%) alloy was obtained by the authors using arc-melting furnace under ultra-pure argon atmosphere, following a procedure well described in the literature [4, 16–18]. The composition was analyzed by EDX and XRF and found to be quite close to the nominal values. Scanning electron microscopy (SEM) analysis revealed surfaces without defects from casting process, while the mapping of Mo shows a homogeneous distribution of this element for Ti–15Mo alloy [8–10] (these data are not given in this paper).

Electrochemical experiments were conducted in a standard three-electrode cell having 0.44 cm^2 of exposed area in the working electrode, with a platinum mesh as a counter electrode and a SCE as reference. These studies were performed in the following naturally-aerated solutions, containing chloride and fluoride ions: (a) 0.15 mol L^{-1} Ringer (8.610 g L^{-1} NaCl, 0.490 g L^{-1} $CaCl_2$ and KCl 0.300 g L^{-1}); (b) 0.15 mol L^{-1} Ringer plus 0.036 mol L^{-1} NaF and (c) 0.036 mol L^{-1} NaF.

The working electrodes (Ti–15Mo alloy and cp-Ti grade 2) were polished with 600 grade silicon carbide paper and rinsed with distilled and deionized (Milli-Q®) water. All experiments were conducted at 25 °C. The E_{oc}, CV and EIS measurements were performed using a potentiostat/galvanostat Solartron Electrochemical Interface mod. SI 1287 and Solartron Instruments HF Frequency Response Analyser, mod. SI 1255.

Open-circuit potential measurements, E_{oc} measurements, E_{oc}, were carried out on freshly-polished samples, in naturally-aerated aqueous electrolytes solutions described above, immediately after polishing. The E_{oc} values were recorded after 0, 1, 24, 48, 72, 168, 240, and 360 h. In order to verify the reproducibility of E_{oc} results, this analysis was repeated three times. The voltammetric analyses were started at a potential in the hydrogen evolution region (−0.8 V vs. SCE) by scanning at 50 mV/s towards more positive potentials up to 8.0 V (SCE), when the scanning was reversed towards the initial potential. The voltammetric profiles were obtained for Ti–15Mo alloy in all electrolytes. Later, experiments were also carried out on different scan rates (1–200 mV s^{-1}). After the potentiodynamic anodizations, the Ti–15Mo surface was analyzed by SEM. EIS measurements were carried out on E_{oc} using a Solartron 1260 electrochemical Frequency Response Analyzer (FRA) system. The impedance spectra were acquired in the frequency range from 100 kHz to 10 mHz with a disturbance signal of 10 mV. EIS plots were obtained after the specimens were immersed in the test solutions for different numbers of hours (1, 24, 48, 72, 168, 240, and 360 h). Each analysis was repeated three times, observing if there was repeatability of the tests.

After 360 h of immersion, the X-ray photoelectron spectroscopy analysis (XPS) was performed using a spectrometer (UNI-SPECS UHV) to analyze the chemical structure of Ti–15Mo alloy, in order to observe possible changes in the chemical composition on the sample surfaces. The line Mg was used (hn = 1,253.6 eV), and the energy step of the analyzer for high resolution spectra was set to 10 eV. From the data experiments the composition of the surface layer (~3 nm) was determined with accuracy of ±10 %, and the error of the peak positions was ±0.1 eV.

3 Results and discussion

Electrochemical studies of the Ti–15Mo alloy were performed using different electrolytic solutions similar to those found in naturally-aerated solutions, and the (cp-Ti grade 2) was used as control.

3.1 Open circuit potential (E_{oc})

An experiment to study the metal stability is to measure the E_{oc}. This spontaneous process allows measuring the time taken to form the oxide film on the sample surface of the

metals or metal alloys, which can protect them against the corrosion [20].

The curves obtained for the variation of E_{oc} versus time for cp-Ti grade 2 and Ti–15Mo alloy in different solutions during 60 min of analysis can be observed in Fig. 1a and b, respectively.

During 60 min of observation, the potential values ranged from −350 to −500 mV in different solutions for the Ti–15Mo alloy in analysis. For the samples of cp-Ti grade 2 in 60 min of analysis, the values ranged from −378 to −625 mV. Similar results were observed by Oliveira and Guastaldi [4], who used several Ti–Mo alloys containing different concentrations of Mo and observed their electrochemical behavior in solutions simulating the physiological media.

It can be observed in Fig. 1a and b that the addition of Mo to titanium increased the protective properties of the titanium oxide, [4, 18]. The potential values increased at the very beginning, and then, the values did not increase significantly after 10 min. Therefore, the spontaneously passivation was still observed (the oxide film is formed spontaneously). Studies on Ti surfaces showed that the composition of oxide film formed spontaneously is mainly TiO_2, and that other oxides can be present, such as TiO, Ti_2O_3, depending on the position of the oxide on the metal surface [21].

In order to check how the values of OCP vary in larger immersion times, analyses were conducted with the Ti–15Mo alloy immersed up to 360 h in all solutions investigated (Fig. 2).

It was found the same behavior for the Ti–15Mo in the largest time of analysis (360 h): potential values increased at the beginning, and then, the values did not increase significantly until 360 h.

The decreasing order of protection against corrosion was, successively, 0.15 mol L^{-1} Ringer, 0.15 mol L^{-1} Ringer plus 0.036 mol L^{-1} NaF and 0.036 mol L^{-1} NaF. The ions Cl^- and F^- reacted chemically with Ti, attacking the sample surface and could have modified the properties of the oxide film formed, leading to values of the open-circuit potentials more negative for the NaF solution than any other solutions (due to presence of F^- ions).

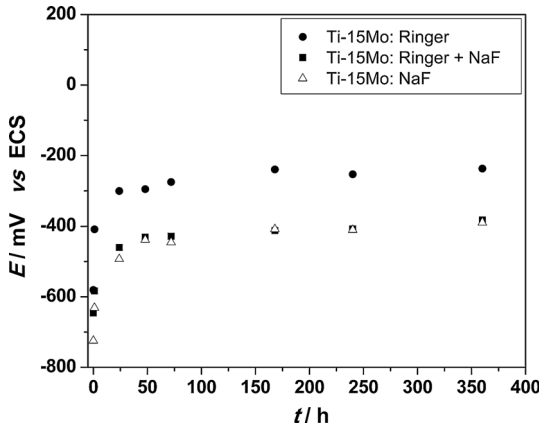

Fig. 2 Open-circuit potential values versus time for Ti–15Mo alloy in different solutions (0.15 mol L^{-1} Ringer, 0.15 mol L^{-1} Ringer plus 0.036 mol L^{-1} and 0.036 mol L^{-1} NaF) up to 360 h

3.2 Cyclic voltammetry (CV)

The cyclic voltammograms obtained for the cp-Ti grade 2 and Ti alloy (Ti–15Mo alloy) in different solutions can be observed in Fig. 3a and b. In all cyclic voltammograms, there was a region of formation and growth of an anodic oxide, and this was observed during the anodic current density increase, where there was not the transpassivation in the Ti–15Mo surface alloy in potentials up to 8 V. In the reverse scan, the current density value was reduced rapidly

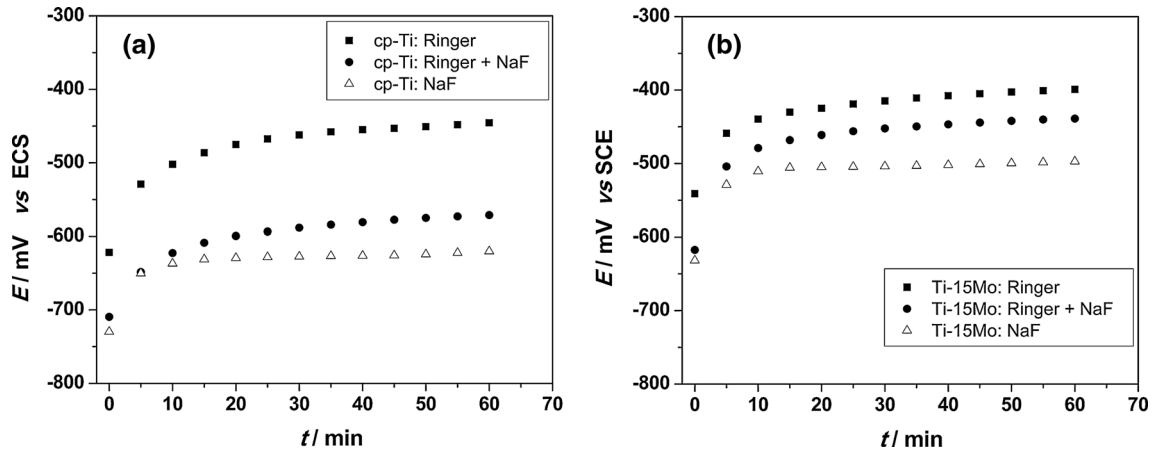

Fig. 1 Open-circuit potential values versus time for **a** cp-Ti and **b** Ti–15Mo, in different solutions (0.15 mol L^{-1} Ringer, 0.15 mol L^{-1} Ringer plus 0.036 mol L^{-1} and 0.036 mol L^{-1} NaF)

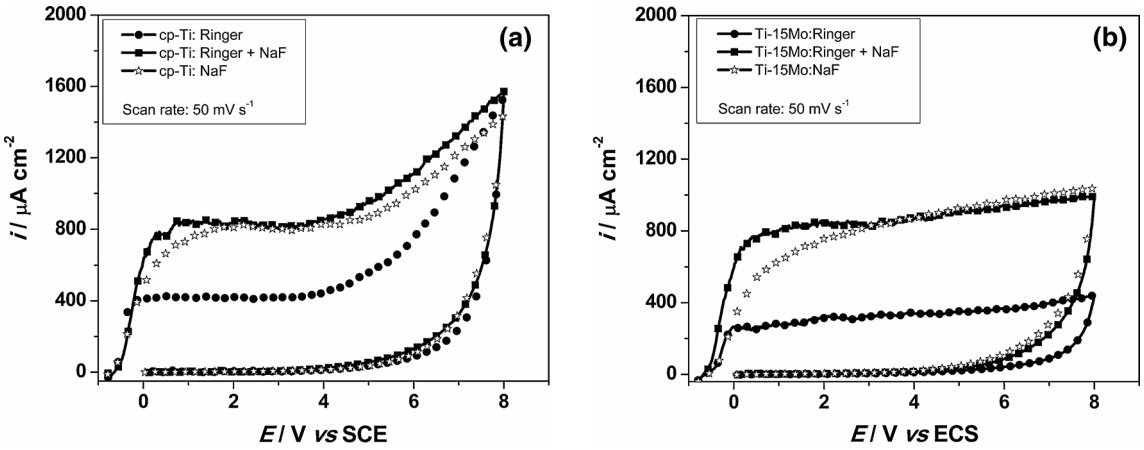

Fig. 3 Cyclic voltammogram for **a** cp-Ti and **b** Ti–15Mo alloy, in different solutions (0.15 mol L^{-1} Ringer, 0.15 mol L^{-1} Ringer plus 0.036 mol L^{-1} and 0.036 mol L^{-1} NaF) to 50 mV s^{-1}

to values close to zero, without reduction of the oxide film formed. There was the passivation of the cp-Ti grade 2 and Ti–15Mo alloy, therefore suggesting stability of the oxide film. Near the region of 4 V, the current density began to increase, indicating that there was a parallel reaction of water oxidation and release of O_2. In literature [4], is described the Pourbaix diagram (Fig. 4) that shows oxidation reactions of the water above 1.2 V, approximately, and, therefore, it can be inferred that close to 4 V in cyclic voltammograms (Fig. 3), there was the release of O_2, since it was observed an increase of the current density, what is thermodynamically possible in some potentials, similar results were observed by Oliveira et al. [17].

The difference between the values of current density of cp-Ti grade 2 and the Ti–15Mo alloy can be explained by the presence of Mo, which is present both on the alloy and on the oxide film surface, which increased the resistance of the alloys against corrosion [15–17].

For the experiments performed in Ringer solution, shown in Fig. 4, the current density values for Ti–15Mo alloy were of 300 µA cm^2, while the value for the cp-Ti grade 2 was 400 µA cm^{-2}. For the Ringer plus NaF and NaF solutions, the current density values increased more than the previous, indicating the corrosion resistance reduction of the samples. According to Kumar and Narayanan [3], there was a negative influence of F^- ions in the corrosion resistance of Ti–15Mo alloy, and these ions are capable of reducing the current density and potential values due to the formation of a porous layer or a defect of the oxide [22]. The presence of F^- ions in neutral solutions did not prevent the formation of a protective layer. Despite this, they influenced some properties of the oxide film formed, and the corrosion of Ti and Ti–15Mo alloy were enhanced in acid environment, as a result of F^- and H^+ ions reaction, forming HF [23].

The next experiment consisted of performing cyclic voltammograms with different scan rates (1, 5, 10, 50, 100, 200 mV s^{-1}). The results obtained for Ti–15Mo alloy in the solution containing 0.15 mol L^{-1} Ringer plus 0.036 mol L^{-1} NaF are presented in Fig. 5. The relation between the current density and the scan rate in the different solutions is shown in Fig. 6. It can be visualized that the anodization rate was not significantly influenced by the presence of Cl^- ions. However, it was affected by the presence of F^- ions, and their anodization rates were higher [17].

The presence of Cl^- ions did not present significant influence in the anodic oxide growth, which was seen when the current density passed through the zero in the beginning of the scan rate. However, this was not observed for F^- ions, because the current density value was higher. Our working hypothesis is that F^- ions would break down the

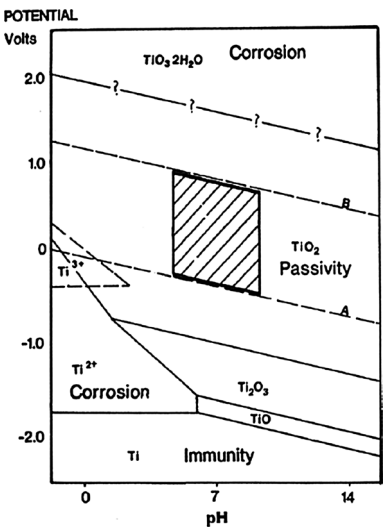

Fig. 4 Pourbaix diagram for Ti

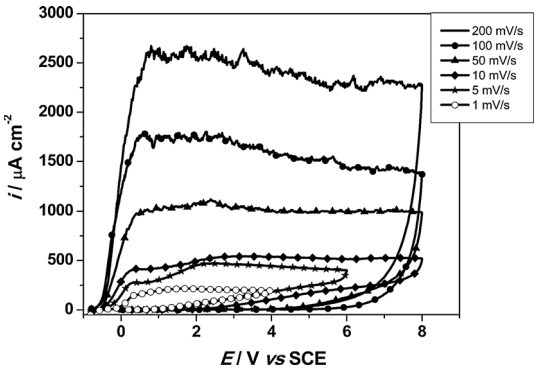

Fig. 5 Cyclic voltammograms for Ti–15Mo alloy in 0.15 mol L^{-1} Ringer plus 0.036 mol L^{-1} NaF for different scan rates

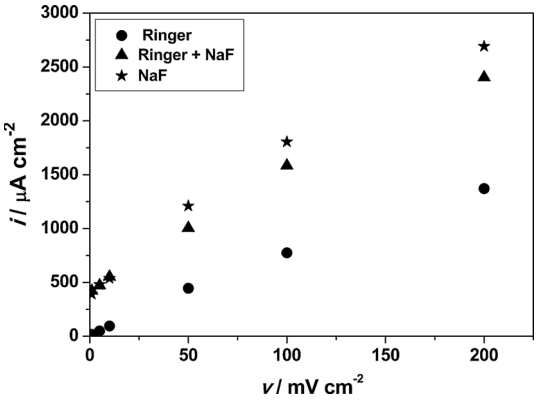

Fig. 6 Current density passive versus scan rate for Ti–15Mo alloy in different solutions

oxide film, and the chemical kinetic of these ions would increase the defective film. All these results are according to and confirm those obtained in the E_{oc} analysis.

3.3 Scanning electron microscopy (SEM)

It was observed the surfaces of the Ti–15Mo alloy in Fig. 7, after anodic oxide growth in different electrolyte solutions during the application of the CV with a scan rate 50 mV s^{-1}. The Ti–15Mo alloy surface without application of the CV was used as control. By the SEM technique, all records of the surfaces were obtained with the magnification of 100×. There was no pitting corrosion on these surfaces (this sort of corrosion is a quite distinct) [24]. These results are according to those observed in CV (Fig. 3a, b).

3.4 Electrochemical impedance spectroscopy (EIS)

Many researchers have been using this technique to prove the influence of the aggressive ions in the dissolution of the protective oxide film formed on the Ti alloys surfaces [3, 4, 13, 14, 16, 17, 23]. The electrochemical corrosion behavior of the Ti alloys in solutions containing Cl^- ions was described by González and Mirza-Rosca [14]. Similar experiments using solutions containing F^- ions were performed by Al-Mayouf et al. [16], and by Mareci et al. [13] utilizing solutions of different pHs, such as acidic pH (2.5) and basic pH (8) [13]. A film that presents high resistance implies its high corrosion resistance, and while a decrease in the passive film capacitance corresponds to a slow growth of the titanium and molybdenum oxides and a long-term stability of the thin passive film [3, 13, 14, 20, 25]. Bode plots and Nyquist spectra can be seen in Fig. 8.

The phase θ and log |Z| versus log *f* are plotted in the Bode Diagram (Fig. 8). The Bode impedance plot revealed that there was a dependence of the impedance values of the presence of F^- and Cl^- ions. The phase θ is an important and sensitive parameter that is used to indicate the presence of additional time constants in the Bode impedance at the highest and at the lowest frequencies [4]. In lower frequencies, 100 mHz (phase θ vs. log *f*), the phase θ indicated that phase angles shift from 50 to 80° with immersing time of the Ti–15Mo alloy in all the solutions. It meant that Rp increased after 360 h of the immersion. However, Rp values were lower in the presence of NaF solution, which

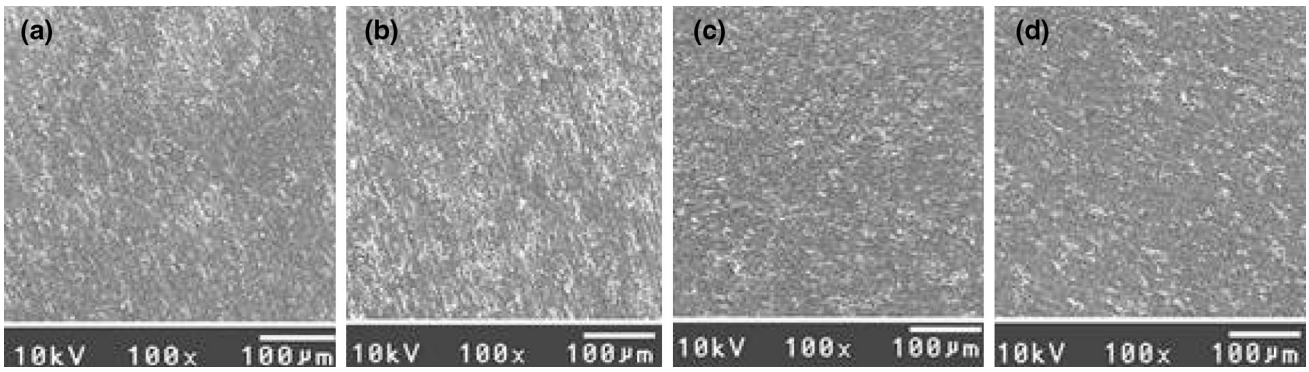

Fig. 7 SEM micrographs for Ti–15Mo alloy polished without application of voltammetry (**a**), and after application of cyclic voltammetry with a scan rate of 50 mV s^{-1} in 0.15 mol L^{-1} Ringer (**b**), in 0.15 mol L^{-1} Ringer plus 0.036 mol L^{-1} NaF (**c**), and in 0.036 mol L^{-1} NaF (**d**) solutions

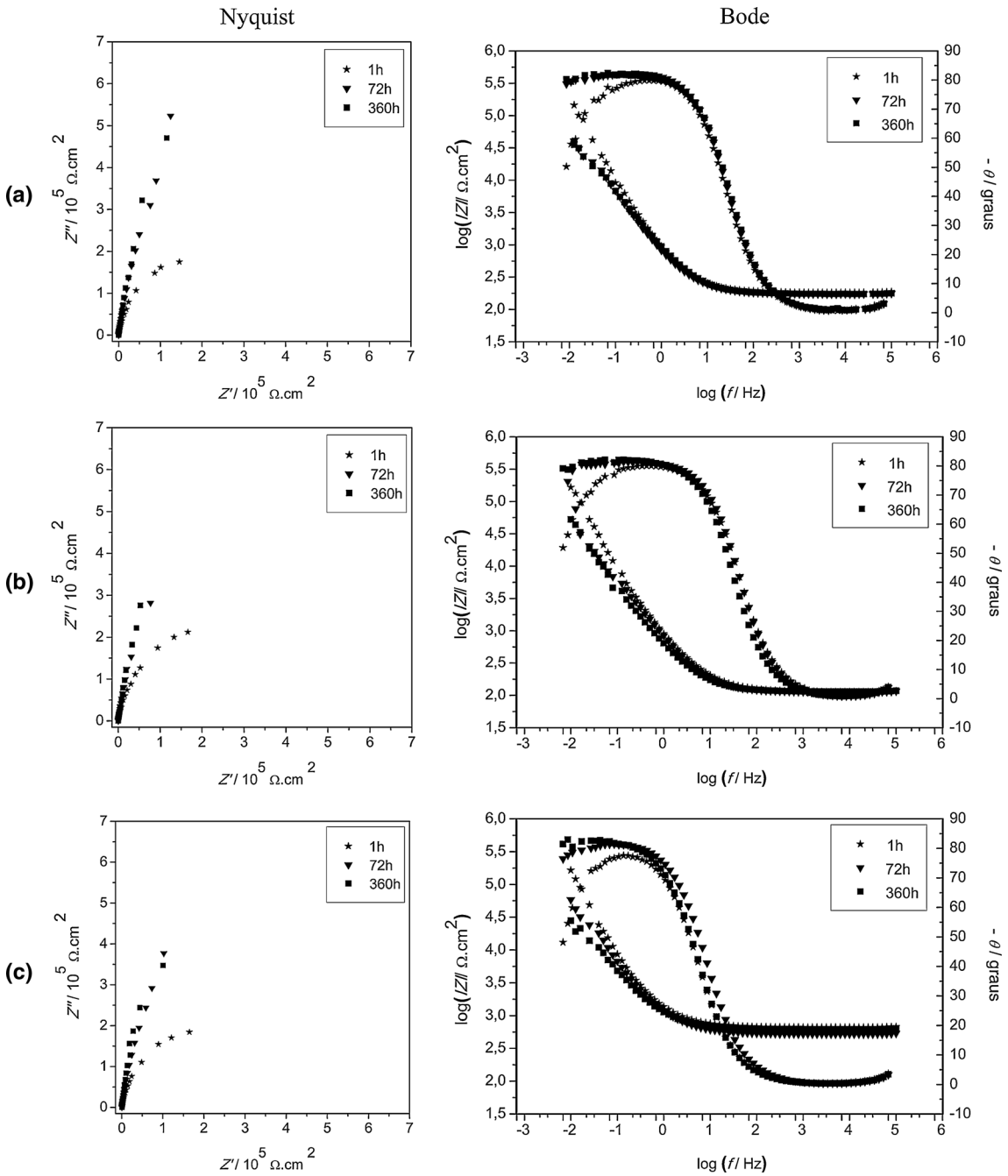

Fig. 8 Nyquist and Bode diagrams for Ti–15Mo alloy after different immersion times in: **a** 0.15 mol L^{-1} Ringer; **b** 0.15 mol L^{-1} Ringer plus 0.036 mol L^{-1} NaF and **c** 0.036 mol L^{-1} NaF solutions

made the formed film to lose its ideal capacitance behavior. In the higher frequencies, 100 kHz (log |Z| vs. log *f*), Rs values were larger in the presence of NaF.

At the present study, a satisfactory fit (Fig. 8, for Ti–15Mo) of all data could be obtained using a simple R_s (QR_p) circuit (Fig. 9), where R_s and R_p are the solution and the parallel (film) resistances, respectively, and Q is a constant phase element (CPE), which takes into account the capacitive behavior of the film [4]. Gonzalez and Mirza-Rosca [14] proposed R_s (QR_p) as the equivalent circuit model to fit the EIS data in the case of a single passive film present on the metal surface. This equivalent circuit has been generally used to fit oxides grown on Ti–15Mo alloy under different situations [4].

The electrical parameters were obtained from fitting data which compared experimental with simulated values [4].

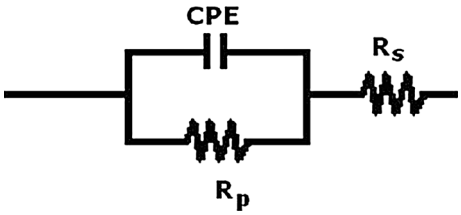

Fig. 9 Electrical equivalent circuit used for the oxides grown on Ti–15Mo alloy

Table 1 Parameters of the electrochemical impedance spectroscopy of the Ti–15Mo alloy after different immersion times in different solutions containing Cl^- and F^- ions

Solutions (mol L^{-1})	Time (h)	Rs/ (Ω cm^2)	Cp/10^{-5} (F cm^{-2})	Rp/10^6 (Ω cm^2)	n
Ringer 0.15	1	182.0	3.5000	0.43149	0.91863
	24	173.4	2.7780	1.7277	0.92415
	48	176.5	2.6614	2.1502	0.92399
	72	173.6	2.6040	3.1690	0.92729
	168	171.2	2.4395	3.8792	0.92611
	240	178.5	2.6250	4.0075	0.92093
	360	174.3	2.5517	4.4169	0.92047
Ringer 0.15 + NaF 0.036	1	113.9	3.6428	0.54461	0.90977
	24	115.2	3.2623	1.8676	0.91808
	48	116.4	3.3086	2.3466	0.91970
	72	112.9	3.5244	2.0979	0.92002
	168	111.0	3.8892	2.1297	0.91785
	240	114.8	4.2400	3.4796	0.91875
	360	114.6	4.4942	3.5801	0.92091
NaF 0.036	1	664.1	4.1296	0.45677	0.90966
	24	678.0	3.5846	1.5836	0.91381
	48	668.1	3.3760	2.0081	0.92042
	72	525.9	3.3784	2.4521	0.92302
	168	613.9	3.8921	3.9587	0.92199
	240	615.7	4.1096	3.3287	0.92280
	360	607.8	4.2169	3.3672	0.92788

According to Table 1, which was constructed from fitting data, Rp values increased with the immersion time, and this high impedance values indicated an improvement in the corrosion resistance of the single and thin film formed spontaneously. This was observed for all solutions. Nevertheless, Rp values decreased when the samples were immersed in solutions containing Cl^- and F^- ions, mainly in the solution containing F^- ions (3.3672×10^6 Ω cm^2). In solutions containing these ions, Cp values were the highest after the immersion time, mainly in solution with F^- ions (4.2169 F cm^{-2}), indicating a possible electro-chemical reaction of the sample in the electrolyte medium and formation of a porous or defective oxide layer whereas the passive region is associated with the formation of one or more protective oxide films [1, 12]. The fact that this behavior did not follow the ideality can be explain by Eq. 1:

$$Cp = \frac{\varepsilon_0 A \varepsilon}{d} \quad (1)$$

ε_0 is the dielectric constant, of vacuum ($8{,}854 \times 10^{-14}$ F cm^{-1}); A is the film surface; ε is the film dielectric constant and d is the film thickness. There was a reduction of d because of the faults in the protective film, and the corrosion products may have caused defects in the oxide film, increasing Cp and decreasing Rp values [4].

Although within same magnitude order, the values variation of Rp confirm the results obtained in E_{oc} and CV techniques: the titanium oxide had a higher resistance against the corrosion in Ringer solution. Although the values of Rp in solutions containing F^- ions are lower, they increased in the beginning of the analyses, did not decrease during the measurements, and the values hardly varied in the last performances. This means that the Ti–15Mo alloy is still resistant to corrosion even in the presence of F^- ions.

3.5 Concentration rate between Ti and Mo from X-ray photoelectron spectroscopy (XPS)

The XPS technique is important and widely used to identify the films formed under Ti alloys, and allows evaluating, for example, their oxide compositions on the Ti–15Mo alloy surfaces [26]. In this work, the concentrations of Ti and Mo as oxide metals were obtained by XPS. The XPS obtained for the Ti–15Mo alloy surface in different solutions can be observed in Figs. 10, 11 and 12.

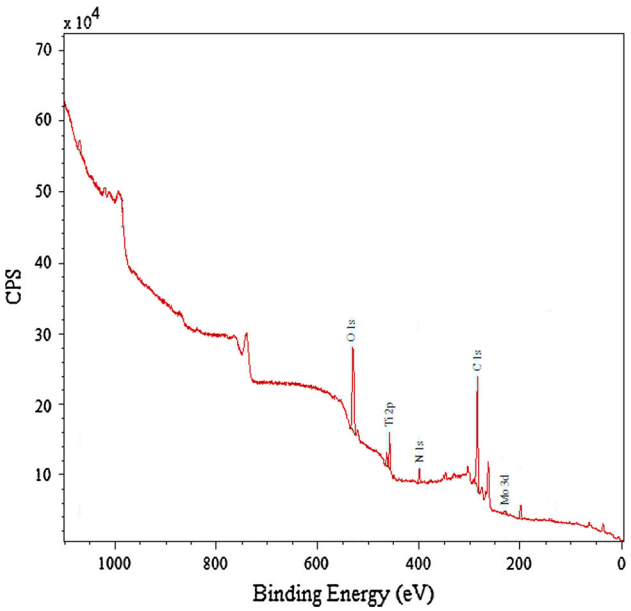

Fig. 10 XPS spectrum for Ti–15Mo alloy surface in Ringer 0.15 mol L^{-1}

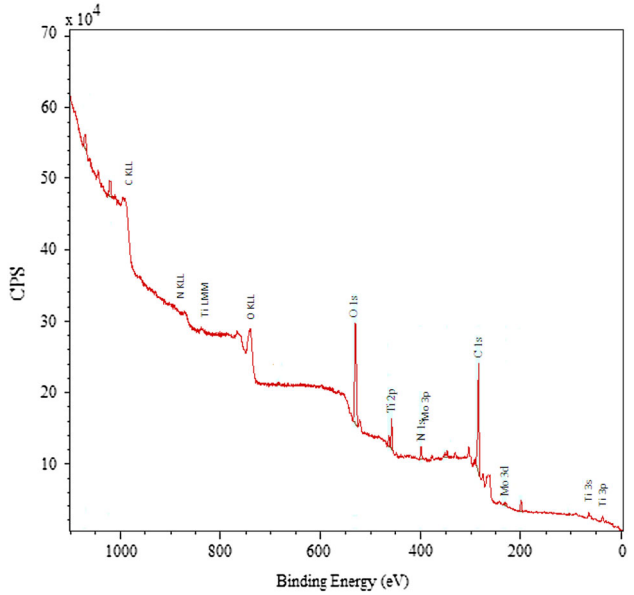

Fig. 11 XPS spectrum for Ti–15Mo alloy surface in Ringer 0.15 mol L^{-1} plus NaF 0.036 mol L^{-1}

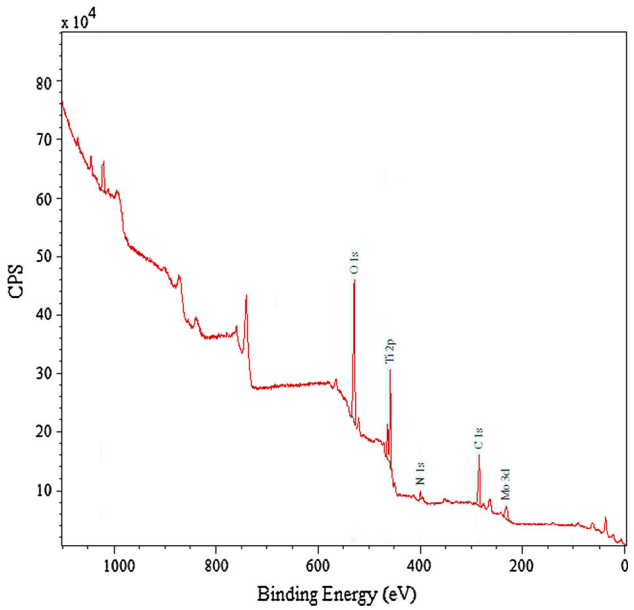

Fig. 12 XPS spectrum for Ti–15Mo alloy surface in NaF 0.036 mol L^{-1}

The Figs. 10 and 12 presented peaks of Ti 2p, C 1s, O 1s, N 1s and Mo 3d, and the Fig. 11 presented peaks of Ti 2p, Ti 3s, Ti 3p, C 1s, O 1s, N 1s, Mo 3s and Mo 3d. On the Ti–15Mo alloy surface, there were elements which formed of the metal alloy, Ti and Mo, besides there were impurities as C, O and N. These impurities are presented on the Ti–15Mo alloy surface due to factors, such as air (these elements are presented in air), preparation of the sample, and cleaning water. The presence of the O 1s and the Ti 2p, Mo 3s, Mo 3d peaks, indicating that there was TiO_2 and MoO_3 on the Ti–15Mo alloy surface. [17]. Comparing the percentages (%) between the Ti and Mo amounts as oxides structures (TiO_2 and MoO_3) on the Table 2, it can be seen that the higher rate was in Ringer (7.6 %), decreasing in Ringer plus NaF (7.2 %) and NaF (4.9 %), respectively. However, the least amount of the alloy elements (Mo) on the surfaces was found in solution containing F^- ions due to the attack of the Ti–15Mo alloy in the passive regions.

Table 2 Ratio between the concentrations of cp-Ti (Ti) and Mo on the Ti–15Mo alloy surfaces immersed in different solutions

Solutions (mol L^{-1})	Rate Ti/Mo (%)
0.15 Ringer	7.6
0.15 Ringer + 0.036 NaF	7.2
0.036 NaF	4.9

4 Conclusion

The exposure of the Ti–15Mo alloy in naturally-aerated solutions, containing chloride and fluoride ions, caused a decrease in corrosion resistance, and the stable passive oxide film was observed in solution containing F^- ions. Micrographs obtained by SEM indicated that there was a homogeneous and uniform region distributed on the surfaces of all the alloys, without pitting corrosion. Results from XPS measurements, indicated presence of the O 1s, Ti 2p, Mo 3s and Mo 3d peaks, showing there were TiO_2 and MoO_3 on the Ti–15Mo alloy surface. Nevertheless, it could be observed a protection against corrosion in the Ti–15Mo alloy surface.

Acknowledgments The authors express their sincere acknowledgements to CNPQ for the scholarship and grant for making this work possible, and Isabela Mascia Silveira for the English revision of the manuscript.

References

1. Kumar S, Narayanan TSNS, Kumar SS. Influence of fluoride ion on the electrochemical behaviour of β-Ti alloy for dental implant application. Corros Sci. 2010;52:1721–7.
2. Nakagawa M, Matsuya S, Udoh K. Corrosion behavior of pure titanium and titanium alloys in fluoride-containing solutions. Dent Mater J. 2001;20:305–14.
3. Kumar S, Narayanan TSNS. Corrosion behavior of Ti–15Mo alloy for dental implant applications. J Dent. 2008;36:500–7.
4. Oliveira NTC, Guastaldi AC. Electrochemical stability and corrosion resistance of Ti–Mo alloys for biomedical applications. Acta Biomater. 2009;5:399–405.
5. Stookey GK. Critical evaluation of the composition and use of topical fluorides. J Dent Res. 1990;69:805–12.
6. Huang HH. Effects of fluoride and albumin concentration on the corrosion behavior of Ti–6Al–4V alloy. Biomaterials. 2003;24:275–82.

7. Nakagawa M, Matono Y, Matsuya S, Udoh K, Ishikawa K. The effect of Pt and Pd alloying additions on the corrosion behavior of titanium in fluoride containing environments. Biomaterials. 2005;26:2239–46.
8. Al-Mayouf AM, Al-Swayih AA, Al-Mobarak NA, Al-Jabab AS. Corrosion behavior of a new titanium alloy for dental implant applications in fluoride media. Mater Chem Phys. 2004;86:320–9.
9. Tavares AMG, Fernandes BS, Souza SA, Batista WW, Cunha FGC, Landers R, Macedo MCSS. The addition of Si to the Ti–35Nb alloy and its effect on the corrosion resistance, when applied to biomedical materials. J Alloys Compd. 2014;591:91–9.
10. Martins DQ, Souza MEP, Souza SA, Andrade DC, Freire CMA, Caram R. Solute segregation and its influence on the microstructure and electrochemical behavior of Ti–Nb–Zr alloys. J Alloys Compd. 2009;478:111–6.
11. Afonso CRM, Aleixo GT, Ramirez AJ, Caram R. Influence of cooling rate on microstructure of Ti–Nb alloy for orthopedic implants. Mater Sci Eng C. 2007;27:908–13.
12. Eisenbarth E, Velten D, Müller M, Thull R, Breme J. Biocompatibility of β-stabilizing elements of titanium alloys. Biomaterials. 2004;25:5705–13.
13. Mareci D, Chelariu R, Gordin DM, Ungureanu G, Gloriant T. Comparative corrosion study of Ti–Ta alloys for dental applications. Acta Biomater. 2009;5:3625–39.
14. Gonzalez JEG, Mirza-Rosca JC. Study of the corrosion behavior of titanium and some of its alloys for biomedical and dental implant applications. J Electroanal Chem. 1999;471:109–15.
15. Robin A, Meirelis JP. Influence of fluoride concentration and pH on corrosion behavior of titanium in artificial saliva. J Appl Electrochem. 2007;37:511–7.
16. Oliveira NTC, Aleixo G, Caram R, Guastaldi AC. Development of Ti–Mo alloys for biomedical applications: microstructure and electrochemical characterization. Mater Sci Eng A. 2007;727:452–3.
17. Oliveira NTC, Guastaldi AC, Piazza S, Sunseri C. Photo-electrochemical investigation of anodic oxide films on cast Ti–Mo alloys. I. Anodic behaviour and effect of alloy composition. Electrochim Acta. 2009;54:1395–402.
18. Oliveira NTC, Guastaldi AC. Electrochemical behaviour of Ti–Mo alloys applied as biomaterial. Corros Sci. 2008;50:938–45.
19. Alves APR, Santana FA, Rosa LAA, Cursino AS, Codaro EN. Astudy on corrosion resistance of the Ti–10Mo experimental alloy after different processing methods. Mater Sci Eng C. 2004;24:693–6.
20. Al-Mayouf AM, Al-Swayih AA, Al-Mobarak NA, Al-Jabab AS. The effect of fluoride on the electrochemical behavior of Ti and some of its alloys for dental applications. Mater Corros-Werkstoffe Und Korros. 2004;55:524–30.
21. Niinomi M. Mechanical properties of biomedical titanium alloys. Mater Sci Eng A. 1998;243:231–6.
22. Leach JSL, Pearson BR. The conditions for incorporation of electrolyte ions into anodic oxides. Electrochim Acta. 1984;29:1271–82.
23. Oliveira NTC, Biaggio SR, Piazza S, Sunseri C, Di Quarto F. Photo-electrochemical and impedance investigation of passive layers grown anodically on titanium alloys. Electrochim Acta. 2004;49:4563–76.
24. Zhang X. The pitting behavior of Al-3103 implanted with molybdenum. Corros Sci. 2001;43:85–97.
25. Lavos-Valereto IC, Wolynec S, Ramires I, Guastaldi AC, Costa I. Electrochemical impedance spectroscopy characterization of passive film formed on implant Ti–6Al–7Nb alloy in Hank's solution. J Mate Sci Mater Med. 2004;15:55–9.
26. Milosev I, Metikos-Hukovic M, Strehblow HH. Passive film on orthopaedic TiAlV alloy formed in physiological solution investigated by X-ray photoelectron spectroscopy. Biomaterials. 2000;21:2103–13.